Active fault segments along the North Anatolian Fault system in the Sea of Marmara: implication for seismic hazard

Luca Gasperini, Massimiliano Stucchi, Vincenzo Cedro, Mustapha Meghraoui, Gulsen Ucarkus, Alina Polonia

Mediterranean Geoscience Reviews (2021) 3:29–44
https://doi.org/10.1007/s42990-021-00048-7

ORIGINAL PAPER

Active fault segments along the North Anatolian Fault system in the Sea of Marmara: implication for seismic hazard

Luca Gasperini[1] · Massimiliano Stucchi[2] · Vincenzo Cedro[1] · Mustapha Meghraoui[3] · Gulsen Ucarkus[4] · Alina Polonia[1]

Received: 10 December 2020 / Revised: 14 January 2021 / Accepted: 18 January 2021 / Published online: 8 March 2021

Abstract

A new analysis of high-resolution multibeam and seismic reflection data, collected during several oceanographic expeditions starting from 1999, allowed us to compile an updated morphotectonic map of the North Anatolian Fault below the Sea of Marmara. We reconstructed kinematics and geometries of individual fault segments, active at the time scale of 10 ka, an interval which includes several earthquake cycles, taking as stratigraphic marker the base of the latest marine transgression. Given the high deformation rates relative to sediment supply, most active tectonic structures have a morphological expression at the seafloor, even in presence of composite fault geometries and/or overprinting due to mass-wasting or turbidite deposits. In the frame of the right-lateral strike-slip domain characterizing the North Anatolian fault system, three types of deformation are observed: almost pure strike-slip faults, oriented mainly E–W; NE/SW-aligned axes of transpressive structures; NW/SE-oriented trans-tensional depressions. Fault segmentation occurs at different scales, but main segments develop along three major right-lateral oversteps, which delimit main fault branches, from east to west: (i) the transtensive Cinarcik segment; (ii) the Central (East and West) segments; and (iii) the westernmost Tekirdag segment. A quantitative morphometric analysis of the shallow deformation patterns observed by seafloor morphology maps and high-resolution seismic reflection profiles along the entire basin allowed to determine nature and cumulative lengths of individual fault segments. These data were used as inputs for empirical relationships, to estimate maximum expected Moment Magnitudes, obtaining values in the range of 6.8–7.4 for the Central, and 6.9–7.1 for the Cinarcik and Tekirdag segments, respectively. We discuss these findings considering analyses of historical catalogues and available paleoseismological studies for the Sea of Marmara region to formulate reliable seismic hazard scenarios.

Keywords North Anatolian fault · Sea of Marmara · Earthquakes · Active fault segments · Marine geophysics · Seismic hazard

1 Introduction

Starting from the Mw 7.6, 1999 Izmit earthquake, which ruptured over 50 km of the North Anatolian Fault (NAF) below the Gulf of Izmit in the eastern Sea of Marmara (Ucarkus et al. 2011; Gasperini et al. 2011a), several marine geological studies were carried out by different international teams. The main objectives of such studies were mapping the active fault strands (Le Pichon et al. 2001; Armijo et al. 2005; Şengör et al. 2014), estimating their slip-rate at the scale of several seismic cycles (Polonia et al. 2004; Gasperini et al. 2011b), and evaluating the effect of major earthquakes in the sedimentary sequence (MCHugh et al. 2006; Beck et al. 2007; Çağatay et al. 2012; Drab et al. 2012, 2015; Yakupoğlu et al. 2019). This effort was preliminary to a

✉ Luca Gasperini
luca.gasperini@ismar.cnr.it

✉ Alina Polonia
alina.polonia@ismar.cnr.it

[1] Istituto Di Scienze Marine, Consiglio Nazionale Delle Ricerche (ISMAR-CNR), Bologna, Italy

[2] Istituto Nazionale Di Geofisica E Vulcanologia, Bologna, Italy

[3] Université de Strasbourg, Strasbourg, France

[4] Geological Engineering Department, Istanbul Technical University, Istanbul, Turkey

reliable seismic risk assessment in the densely populated Istanbul Metropolitan Area, considered a "seismic gap" close to the next rupture (Hubert-Ferrari et al. 2000; Bohnhoff et al. 2013; Lange et al. 2019). To foster these studies, the Sea of Marmara was included among the strategic sites for monitoring active faults and exploring seismic precursors within some E.C. initiatives, including MarmEsonet (Geli et al. 2009) and Marsite (Meral Ozel et al. 2013).

Despite the large amount of data and a number of papers that shed light on the tectonic setting of this seismically active region, there are still uncertainties and debates, particularly concerning modes of fault segmentation and nature of each individual segment.

Regarding the overall tectonics of the Sea of Marmara, Barka and Kadinsky-Cade (1988), Barka (1992) and Wong et al. (1995), proposed a pull-apart classic model, with two major strike-slip NE–SW faults delimiting the whole basin. These faults would have been connected by systems of *en échelon* normal faults bounding individual basins. Subsequently, Parke et al. (2002), Okay et al. (2000), Amijo et al. (2002), Meghraoui et al. (2012) suggested the presence of an oblique segmented shear zone connecting the eastern Izmit segment to the Ganos Fault, at the western side of the Sea of Marmara (Fig. 1).

To determine whether and to what extent a fault system is segmented is important. In fact, segmentation reflects structural and geometrical characteristics of continental faults and plate boundaries, where large earthquakes ruptures are limited by major tectonic discontinuities (Wesnousky 2006). Fault segments follow coseismic faulting, with rupture initiation and termination often displaying a pattern of cumulative deformation. This deformation zone is characterized by partitioning over various fault branches at the plate boundary and contributes to the formation of compressional or extensional structures in correspondence of restraining and releasing bends, respectively. This behavior should also be controlled by changes in fault geometries and block rotations, as also suggested by analog modelling in the Sea of Marmara (Bulkan et al. 2020).

According to other authors (Aksu et al. 2000; Le Pichon et al. 2001; Şengör 2003), the northern branch of the NAF consists of a single main fault with a predominantly strike-slip component, the so-called Main Marmara Fault.

Some of these reconstructions were performed before the acquisition of the high-resolution marine geophysical/geological dataset which immediately followed the 1999 Izmit earthquake. Starting from that event, several oceanographic cruises were carried out in the Sea of Marmara, including Marmara 2013, where new high-resolution multibeam and seismic reflection data were collected (Gasperini et al. 2013).

The aim of this paper was to examine geometry and kinematics of the NAF in the Sea of Marmara, as well as the nature and degree of activity of the segments identified

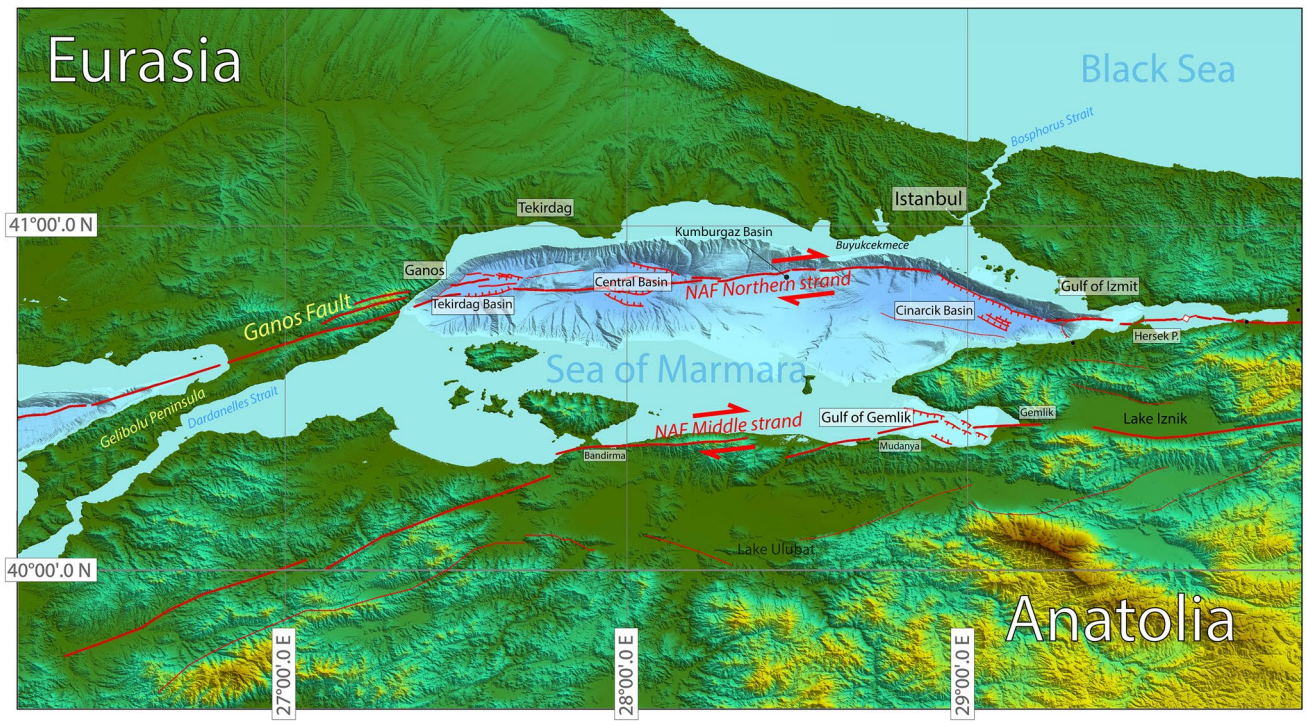

Fig. 1 The North Anatolian Fault in the Sea of Marmara Region (modified from Gasperini et al. 2011b). The black dots represent the estimated location of earthquake epicenters based on historical accounts (see text)

by the transfer zones (bending or overstep), and compile a map which includes structural style and length of active fault segment, with the final aim of estimating their seismic potential. Such findings are discussed considering available information on historical seismicity, which is particularly rich and extended back in time (1000–2000 years), as well as paleoseismological studies carried out underwater (see next sections). We also took advantage by the peculiar stratigraphy of the Sea of Marmara, which allows a relatively robust recognition, and correlation in the whole basin, of a seismostratigraphic marker corresponding to the end of the latest marine ingression, about 12.5 ka (Çağatay et al. 2000, 2003), marked by a − 85 m paleo-shoreline in the Gulf of Izmit, drowned after 10.5 ka (Polonia et al. 2004). To compile a new neotectonic map of the NAF in the Sea of Marmara using available high-resolution marine geophysical data, we made the following assumptions: (i) faults not active during the Holocene (10 ka) are not considered seismogenic; (ii) geometry of the faults observed in shallow seismic profiles (the only available in densely spaced grids for the entire basin), which image the first 30–40 m of sediments, are representative of the kinematics at the scale of the lithosphere due to the peculiarity of strike-slip sub-vertical faults; (iii) the plan-view, 2D morphometric analysis of the faults is representative of their 3D mechanical behavior.

2 The Sea of Marmara

The Sea of Marmara (Fig. 1) is an epicontinental basin, which separates the Black Sea from the Aegean Sea through the Strait of Bosporus and the Dardanelles, respectively. It reflects transtensive deformations at the western end of the NAF (Barka 1992), a major continental transform fault representing the boundary between two major lithospheric plates, Anatolia and Eurasia, which while approaching the Sea of Marmara splits into three main branches (Fig. 1). Geodetic measurements and models suggest a relatively high (22–26 mm/year according to McClusky et al. 2001; Reilinger et al. 2006; Ergintav et al. 2014) right-lateral strike-slip deformation between the two plates, mostly (about 80%, according to Flerit et al. 2003) taken up along the northern branch. All such GPS models describe the relative Anatolia-Eurasia motion as rotating clockwise progressively from E to W along the NAF principal displacement zone in the Sea of Marmara. This results in the incipient formation of a rapidly subsiding pull-apart system (Armijo et al. 2002, 2005).

The bathymetric map of the Sea of Marmara (Fig. 1) shows a complex morphology, with steep slopes and deep basins separated by topographic highs, particularly concentrated along the northern coast (Le Pichon et al. 2001). Three deep topographic depressions, reaching 1200 m below the sea level, and named from east to west, Cinarcik, Central, and the Tekirdag basins, represent the main depocenters.

Even though tangible evidence of coseismic ruptures at the seafloor is lacking, being only limited to the eastern and western edges of the basin (e.g., Armijo et al. 2005; Gasperini et al. 2011a), it is generally assumed that the eighteenth century sequence ruptured entirely the NAF below the Sea of Marmara, which is thus accumulating tectonic load (Hubert-Ferrari et al. 2000; Parsons et al. 2000; Parsons 2004; Rockwell et al. 2009). This interpretation disagrees with the Ambraseys and Jackson (2000) suggestion of a much longer quiescence interval in Central and Western Marmara.

The stratigraphic evolution of the Sea of Marmara is controlled by a complex paleoceanography. Detailed studies of the Holocene marine ingression in Marmara (Eriş et al. 2007; McHugh et al. 2008; Çağatay et al. 2009; Gökaşan et al. 2010; Vidal et al. 2010) enabled to reconstruct the timing of marine reconnection after the Last Glacial Maximum (LGM). During the LGM, the shelves were exposed to subaerial erosion, which reached below the shelf break in most sectors of the Sea of Marmara (Çağatay et al. 2009) creating a characteristic unconformity. Subsequently, beginning from the last interglacial (MIS 1–12 ka) and following a rapid increase in the average global sea level, the Sea of Marmara was reconnected to the Mediterranean, when it reached up to the Dardanelles sill (Çağatay et al. 2000, 2003; Sperling et al. 2003; Eriş et al. 2007). Despite small uncertainties on its timing, the latest Sea of Marmara–Mediterranean reconnection left a clear and well-documented stratigraphic marker in the sedimentary sequence, which could be correlated over the entire basin using high resolution seismic reflection profiles.

2.1 Historical earthquakes

The earthquake history of the Marmara Region is well known, due to special historical circumstances, including the presence of an important city as Byzantium (later Constantinople, now Istanbul). However, assessments of the earthquake location and magnitude suffer from a lack of reports from the southern Marmara coast, characterized by less important settlements. Moreover, the main observation points were clustered in the western and eastern edges of the basin.

For the Sea of Marmara Region, Ambraseys (2002) describes six events with $Mw \geq 7.0$, which took place in 1509, 1719, 1754, 1766 May, 1766 Aug, and 1894. Parameters obtained for such earthquakes by a fully repeatable and transparent approach are those of Parsons (2004), who first assessed macroseismic intensities from information reported in (Ambraseys and Finkel 1990, 1991,1995), applying the method by Bakun and Wentworth (1997) and using

attenuation relationship by Ambraseys (2002). This method allows determining offshore epicenters and, therefore, bettering estimates of the *M* value. It is worth noting that Parsons (2004) also published intensity data points, which can be thus verified. The SHEEC catalogue (Stucchi et al. 2013) provides earthquake parameters obtained also by means of a repeatable method (i.e., Boxer, by Gasperini et al.1999, 2010); in this case, intensity data were available through AHEAD, https://www.emidius.eu/AHEAD, and calibrating coefficients were determined for the Aegean area (Gomez Capera et al. 2009). More recently, Bulut et al. (2019) provided new Mw estimates based on the Bakun and Wentworth (1997) method from newly determined intensity data.

Table 1 shows the ranges of *M* values for the main historical events (from that of 1509 C.E.) as determined by these authors; note that Ms and Mw can roughly be assumed equivalent in the magnitude range considered.

Concerning epicenter locations, it has to be considered that, in case of large earthquakes, they might not be fully representative of the rupture area. Ambraseys (2002) point out that "locations at sea are inferred from macroseismic observations and fault positions", the latter constrained at that time by poor geological-geophysical information at sea. Many investigators prefer to give results directly on map, or associate earthquakes to given fault segments (see for instance Atakan et al. 2002; Parsons 2004; Bulut 2019), although position and kinematics of fault segments are not univocally agreed.

2.2 Submarine paleoseismology

Underwater paleoseismic studies in the Marmara Region include slip-rate estimates and analysis of the earthquake record in sediment cores, at the scale of the last 10 ka (Polonia et al. 2002).

By analyzing displaced geomorphic features, Polonia et al. (2004) and Gasperini et al. (2011b), measured a 10 mm/years right lateral strike-slip rate on both sides of the Marmara fault system, i.e., in the Gulf of Izmit, to the east, and the Gulf of Saros (NE Aegean Sea) to the west, during the Holocene. Such estimate, whose implication are discussed also in Gasperini et al. (2018), is about half of those determined by geodetic observation at the scale of the past decades (Flerit et al. 2003).

Sedimentary records of historical and/or recent earthquakes, including those of the devastating 17 Aug 1999 İzmit earthquake (Mw = 7.6) and 9 Aug 1912 Ganos-Mürefte earthquake (Mw 7.4), were studied in cores collected from the shallow İzmit Gulf, and also in the deeper Tekirdag, Central, Kumburgaz and Cinarcik basins (McHugh et al. 2006; Çağatay et al. 2012; Drab et al. 2012, 2015; Yakupoğlu et al. 2019). The earthquake records are represented by seismo-turbidites that contain commonly a basal coarse layer, a middle-laminated silt layer, and an overlying homogeneous mud layer with peculiar compositional characters that allow distinguishing co-seismic sedimentation from background sediments. The thickness and areal distribution of such seismically triggered deposits might provide useful indirect insight into the magnitude of past earthquake.

The archive of seismically induced turbidites and sediment deformation observed on seismic profiles close to the fault rupture (sand injections, reflectors offset, etc.) was used to identify near field and far field effects of each seismic event. The depocenters of the larger basins contain a record of all major historic earthquakes, such as the 181, 740, 1063, 1343, 1509, 1766, 1894, 1912 C.E. events, found primarily in those basins adjacent to the rupture. Some of these earthquakes, however, were recorded in more than one basin, as for example the 1912 C.E., earthquake recorded both in the Ganos and Saros basins (Aksoy et al.2010), the 740 C.E., recorded in the Central, Kumburgaz and Izmit basins, and the 1509 C.E., recorded in the Kumburgaz and Izmit basins. Independent observations based on turbidite paleoseismological studies suggest that uncertainties related to epicenter location for some historical earthquakes may be high, in agreement with historical reports. The 865 C.E. and 740 C.E. earthquakes located close to İstanbul on the basis of (not well constrained) historical reports could have had effects extending well into the İzmit Gulf; others assigned to İzmit area (e.g., the 1719 C.E. earthquake) may have their epicenter further east of İzmit (Çağatay et al. 2012).

Table 1 Magnitude estimate and approximate location of major historical earthquakes in the Sea of Marmara region according to different sources

Date	Ambraseys (2002) (Table 1) Ms	Parsons (2004) Mw	SHEEC (2013) Mw	Bulut et al (2019) (Table 1) Mw
1509.09.10	7.2	7.4	7.1 ± 0.33	
1719.05.25	7.4 ± 0.35	7.4	6.7 ± 0.30	7.5
1754.09.02	6.8 ± 0.5	7.0	6.9 ± 0.30	
1766.05.22	7.1 ± 0.5	7.2	6.8 ± 0.38	7.3
1766.08.05	7.4 ± 0.35	7.6	7.1 ± 0.34	7.4
1894.07.10	7.3 ± 0.35	7.0	6.7 ± 0.44	–

3 Methods

Our morphostructural synthesis is based on multibeam bathymetric maps and high-resolution seismic reflection profiles collected during several oceanographic expeditions in the Sea of Marmara, including MARMARA-2001; 2005; 2011; 2013 and other cruises onboard of French ships. The map of Fig. 2 shows the coverage of seismic reflection and multibeam data.

Multibeam morphobathymetric data derive from two main sources: (i) the Sep 2000 Ifremer cruise onboard of the R/V Le Suroit, which obtained a 25 m bathymetric grid widely used by several works during the past 20 years (Fig. 2b); (ii) an unpublished 5 m grid (Fig. 2c) collected onboard of the Italian R/V Urania in 2013 (technical details in Gasperini et al. 2013). Although the coverage of the latter dataset is lower, resolution is higher, enabling a more detailed mapping of active tectonic structures showing a morphological expression. Figure 3 reports a comparison of both grids in the central Sea of Marmara. Prior to fault mapping, seismic reflection profiles were analyzed to identify the reflector corresponding to the latest marine/lacustrine transition. While this is a relatively easy task on the shelves, where the reflector is marked by a sharp erosional unconformity, it is more difficult to detect in conformable deeper layers, within the depocenters or along the slopes. For this reason, seismic data interpretation in deep water was referred to available seismo-stratigraphic reconstructions based on the study of sediment cores (e.g.,

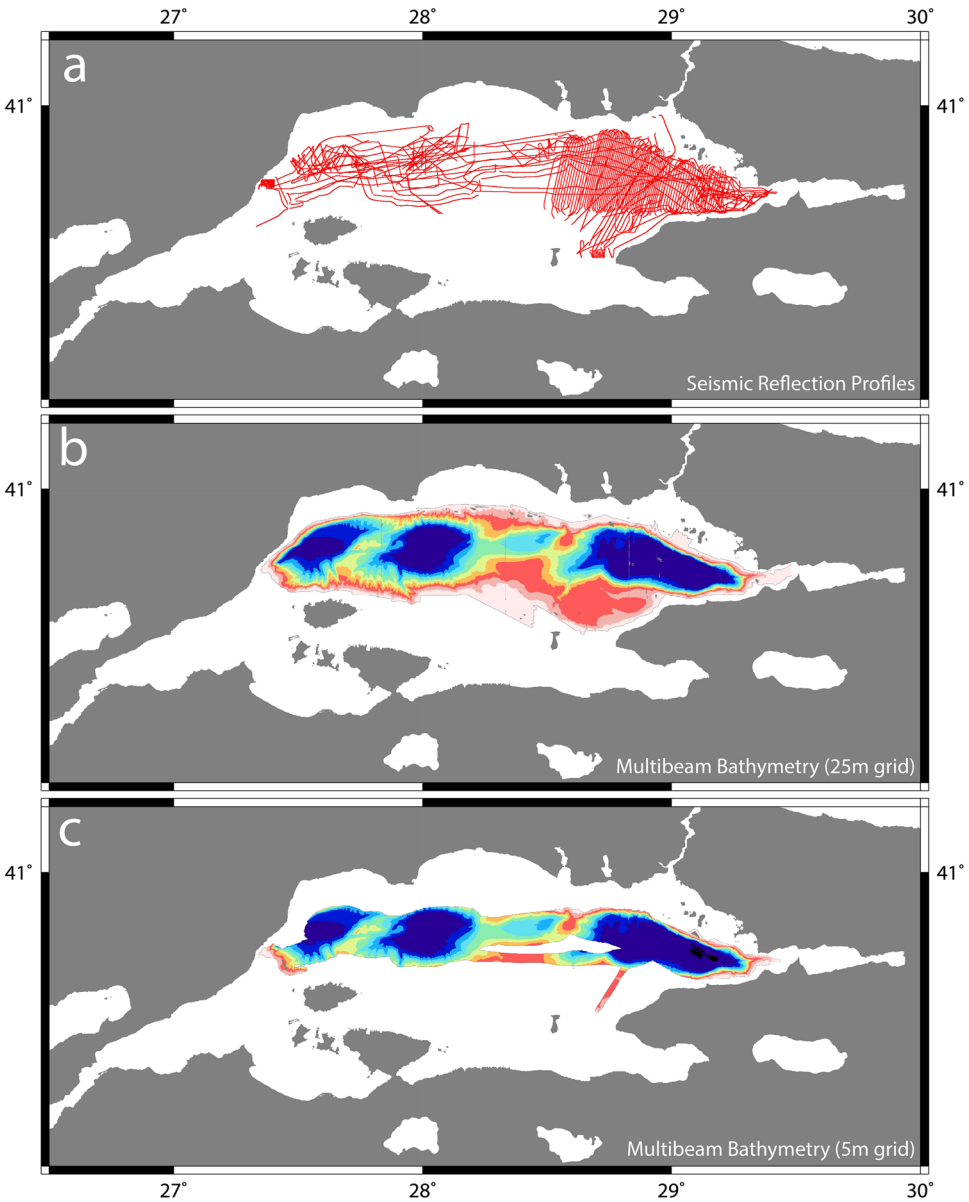

Fig. 2 Bathymetric and seismic reflection data collected during different oceanographic cruises (see text) used for morphostructural reconstructions in this work. **a** Tracks of seismic reflection profiles, **b** 25 m bathymetric grid, **c** 5 m bathymetric grid

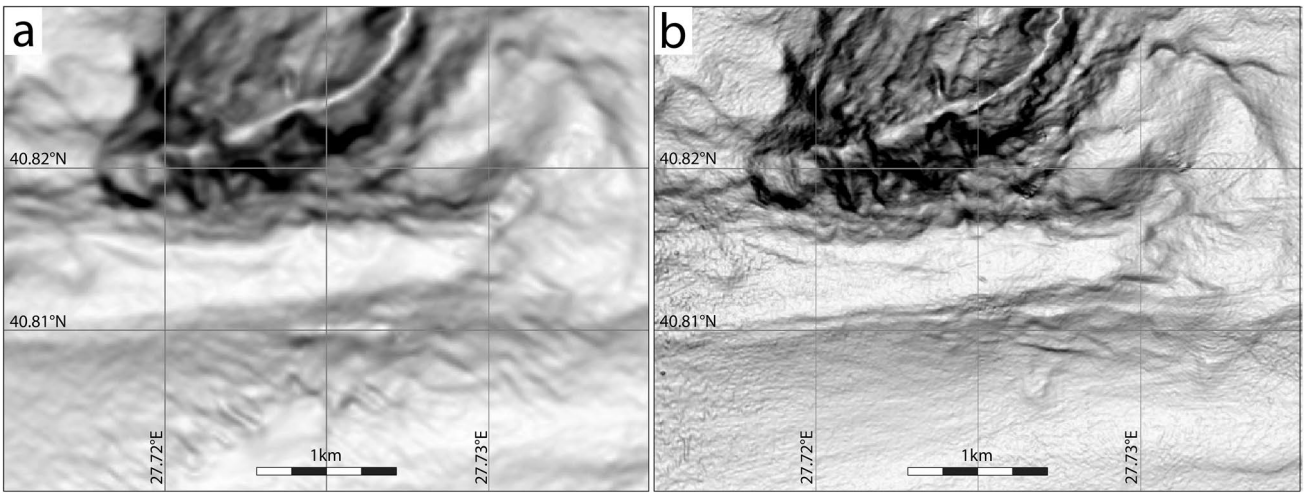

Fig. 3 Comparison between slope maps of the Sea of Marmara floor using two different datasets; **a** data from 2001 Le Suroit cruise (Le Pichon et al. 2001), **b** data from MARMARA 2013 cruise (Gasperini et al. 2013)

Polonia et al. 2004) and correlations with synthetic seismograms (Dal Forno and Gasperini 2008).

Picking of fault segments, often discontinuous in morpho-bathymetric images and shallow seismic reflection images, was carried out using SeisPrho (Gasperini and Stanghellini 2009), obtaining georeferenced vectors subsequently plotted on top of bathymetric slope maps and/or used to compile rose diagrams to analyze orientations. All rose diagrams are divided in three sectors, according to prevailing nature of deformation (strike-slip, transtension, transpression), since orientation of the faults, in relation with small circles defining the Anatolia-Eurasia relative motion is the primary controlling factor of deformation styles.

All maps and graphs were compiled using the free package GMT (Wessel and Smith 1991).

4 Results and interpretations

4.1 Fault patterns

All available morpho-bathymetric and seismo-stratigraphic data were used to compile a new high-resolution morpho-structural map of the NAF northern strand of the Sea of Marmara floor (Fig. 4).

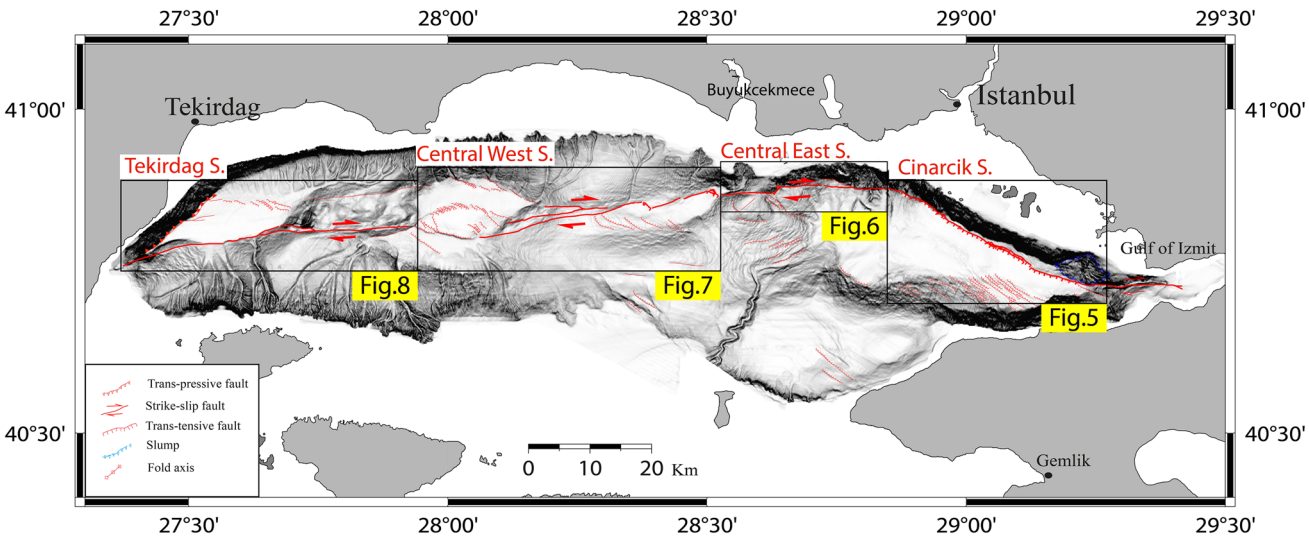

Fig. 4 Morphotectonic map of the North-Anatolian Fault in the Sea of Marmara compiled using available bathymetric and seismic reflection profiles (see text for details)

In all sectors along the NAF principal displacement zone we observe three different styles of deformation: (i) almost pure strike-slip, oriented E-W; (ii) trans-tensional, NW–SE oriented, which is the most common pattern; (iii) trans-pressive structures whose axis is NE-SW oriented. At the scale of the entire Sea of Marmara, 3/4 major segments were identified, corresponding to the main sedimentary basins, the Cinarcik, Kumburgaz, Central and Tekirdag basins, formed along major oversteps or bending (Fig. 4).

The main fault segments observed are, from E to W: (i) the Cinarcik Segment, located east of Istanbul; (ii) the Central East and West segments, located parallel to the coastline immediately south and west of Istanbul; (iii) the Tekirdag Segment, which connects the Central Basin to the western coast of the Sea of Marmara, and then to the Ganos Fault onshore. Concerning the Central East and West segments, separated by two minor oversteps (less than 1 km wide) and a sharp change in orientation, we considered two alternative scenarios, either a single rupture of each of the segments, or a cumulative rupture in the course of a single event.

The Cinarcik segment (Fig. 5) is formed by a N296° striking fault running along the northern continental slope and by a typical transtensional pattern delimited towards the south by *en échelon* antithetic fault segments. Although the deformation zone appears wide and complicated by the presence of overprinting of mass failures due to gravitative instabilitity, it is clear from both seismic reflection profiles and morpho-bathymetric images that the master fault accommodates mainly extension (Fig. 5). This kinematic also accounts for the high topographic gradients and mass flows and sediment remobilizations, detected both in seismic reflection lines and morphobathymetric maps. The prevailing transtensive character of the faults is highlighted in the rose diagram of Fig. 5, by orientations populating mostly the sector between 90° and 180°.

The map in Fig. 4 shows two oversteps and a major change of orientation offshore Buyukcekmece, to the west of Istanbul (Figs. 6, 7). Previous interpretations considered a single fault segment (the Central Segment) connecting the Cinarcik and Tekirdag basins. In this work, based on morphological and seismostratigraphic evidence, we prefer divide the Central Segment into two segments; we called them the Central East and West segments. Insets included in Figs. 6, 7 show how such oversteps are visible by analysis of the 5 m morphobathymetric grid.

The Central East segment (Fig. 6) shows N80°–90° trending strike-slip faults, N250°–N300° extensional faults, representing minor components mainly due to gravitative collapse, and a sharp transpressive overstep close to the termination of the segment. A major compressive topographic high is observed south of the NAF main trace in the western part of the Central East segment (Fig. 6), the so-called Central High. Although the shallow penetration of seismic profiles does not allow a comprehensive analysis of such feature, we observe that it is displaced by the NAF principal deformation zone, which corresponds to a depressed area bounding the northern flank of a bathymetric high. For this reason, we suggest that this feature is presently inactive.

The Central West segment (Fig. 7) is characterized by two prevailing fault patterns. The longer segments, generally oriented N260°–N270° accommodate mainly strike-slip deformation, while the shorter segments, oriented N290°, show transtensional kinematics causing the formation of the topographic depressions. This is the case of the Kumburgaz Basin, in the eastern side of the area, and the Central Basin, a wide rhomb-shaped depression formed by a nested pattern of transtensional faults. In Kumburgaz, the tectonic deformation is controlled by NW–SE extensional faults dipping towards the depocenter, and by NE–SW fault segments with predominantly transcurrent kinematic, that bound the northern edge of the basin. On the NW and SE edges of the Central Basin, extension is accommodated by a series *en échelon* extensional short fault segments. We note that the rhomb-shaped Central Basin constitutes a major overstep which separates the Central West segment from the Tekirdag segment to the west.

The Tekirdag segment (Fig. 8) shows a predominantly strike-slip, with E–W trending faults. The NAF principal deformation zone runs south of the Tekirdag rhomb-shape basin that shows a rather continuous trend if we exclude a very minor bending as it passes from the Western High to the deeper basin (Fig. 8). To the west of 27°30′ E longitude, the fault trace is partially covered by slump deposits, which, however, cut the entire sedimentary sequence up to the seafloor (Fig. 8). We note that the Tekirdag segment is connected without major oversteps, but through a minor bend to the Ganos Fault onshore. A seismic section through the Tekirdag Basin (Fig. 8) shows that, in contrast with the Central Basin, it is markedly asymmetric, with the depocenter running along the base of the southern continental scarp. Holocene and deeper layers show fanning and growth structures, which indicate that part of the deformation is accommodated by extension (transtension). It is interesting to note that the main transtensional segment, which includes the NAF principal displacement zone, is located at the southern edge of the basin, and dips towards the N–NW, antithetically relative to the Cinarcik segment. Extension is also accommodated by a series of minor antithetic extensional segments located on the northern edge of the Tekirdag basin. Transpressional deformations are observed at the base of the western slope.

4.2 Evaluating seismogenic potential

The newly compiled morphotectonic map of Fig. 4, and the close-up views of high- resolution seismic sections

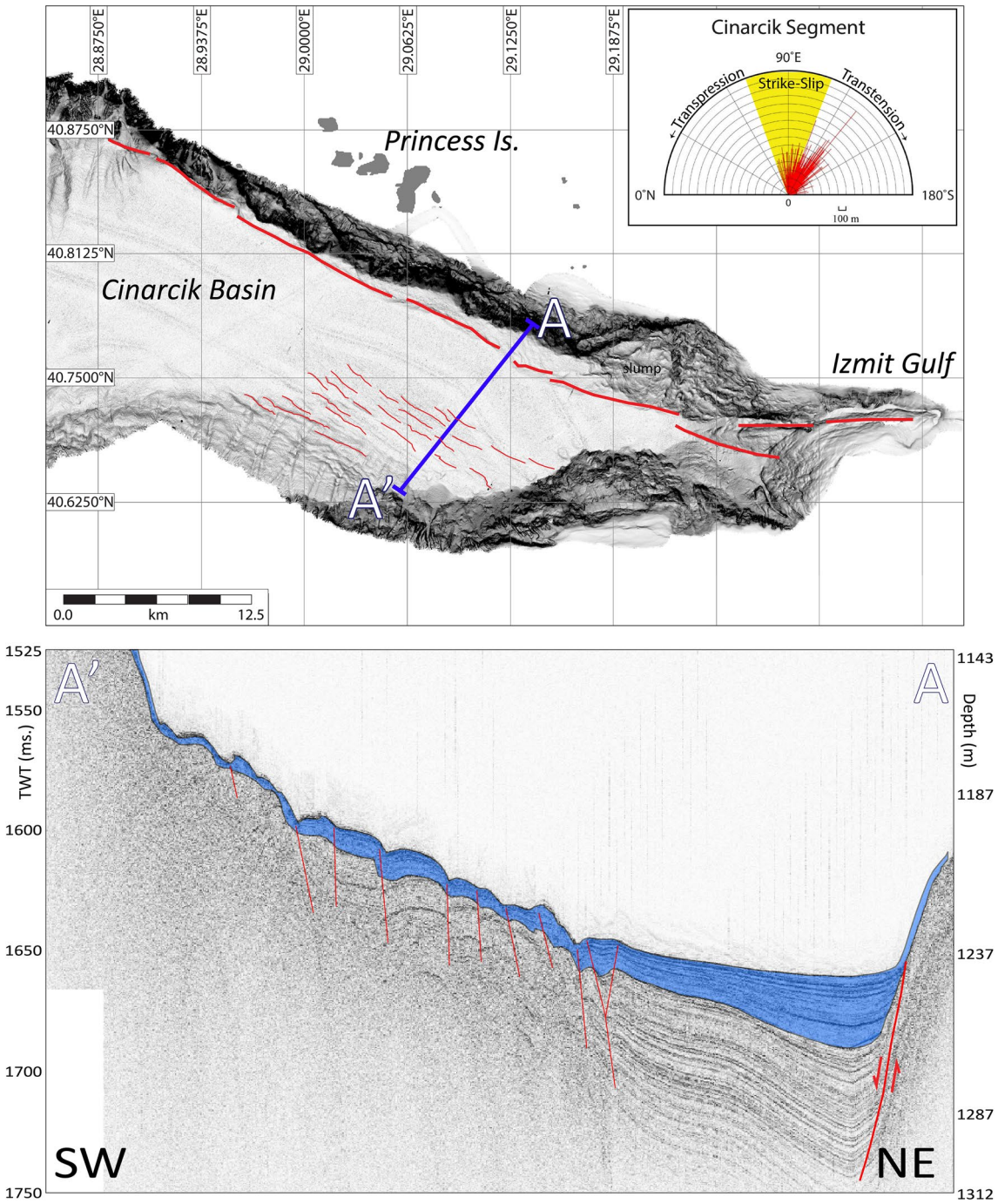

Fig. 5 Morphostructures along the Cinarcik Segment. Top: slope-map of the seafloor obtained using high-resolution morphobathymetric data, with main active faults indicated (red coded lines); inset includes a rose-diagram representing active fault segments orientations. Bottom: high resolution seismic reflection profile (section A-A' in map) with Holocene sediments (pale-blue pattern) and active fault segments indicated

across the NAF principal displacement zone (Figs. 5, 6, 7, 8), highlight different structural settings and geometries along the fault system, suggesting the presence of several individual active segments below the Sea of Marmara, separated by complex areas where deformation is more diffuse. Morphometric and structural analyses enabled us to estimate a maximum expected earthquake magnitude for each of the inferred segments using empirical laws, with an approach similar to that of Bohnhof et al. (2016) for the entire NAF.

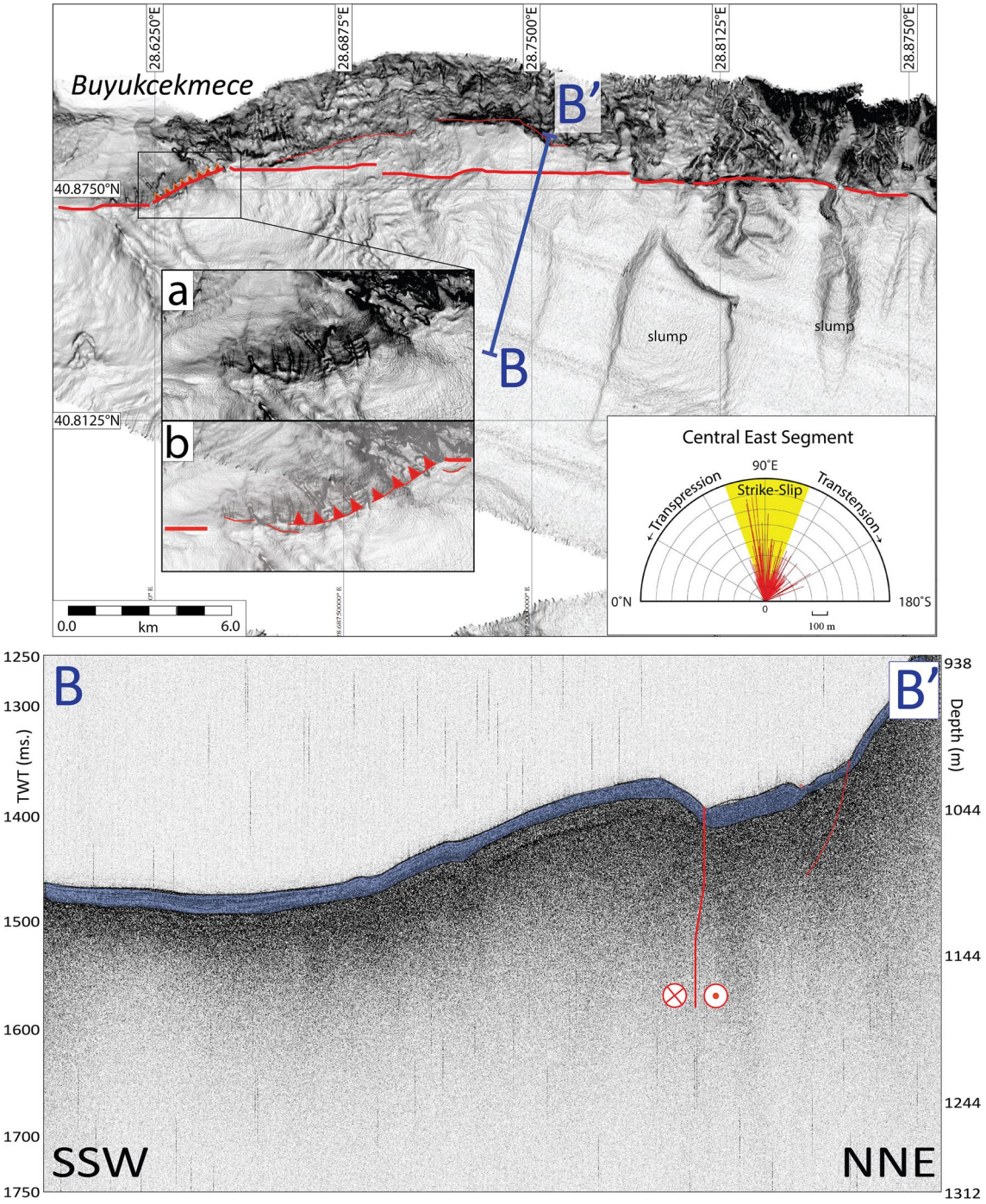

Fig. 6 Morphostructures along the Central East Segment. Top: slope-map of the seafloor obtained using high-resolution bathymetric data, with main active faults indicated (red coded lines); inset includes a rose-diagram representing active fault segments orientations. Bottom: high-resolution seismic reflection profile (section A-A' in map) with Holocene sediments (pale-blue pattern) and active fault segments indicated. Insets include a close up view of the seafloor morphology **a** with main fault tracks **b**

For this purpose, the Wells and Coppersmith (1994) empirical relationships were chosen. A major assumption of such methods is that slip on the fault plane at seismogenic depths is manifested by similar displacements at the surface. This should be in fact the case of strike-slip faults, where coseismic slip is mostly parallel to the fault strike, and rupture is supposed to cut through the uppermost deposits and the entire lithosphere, where they may eventually split into more composite geometries due to changes in rheology.

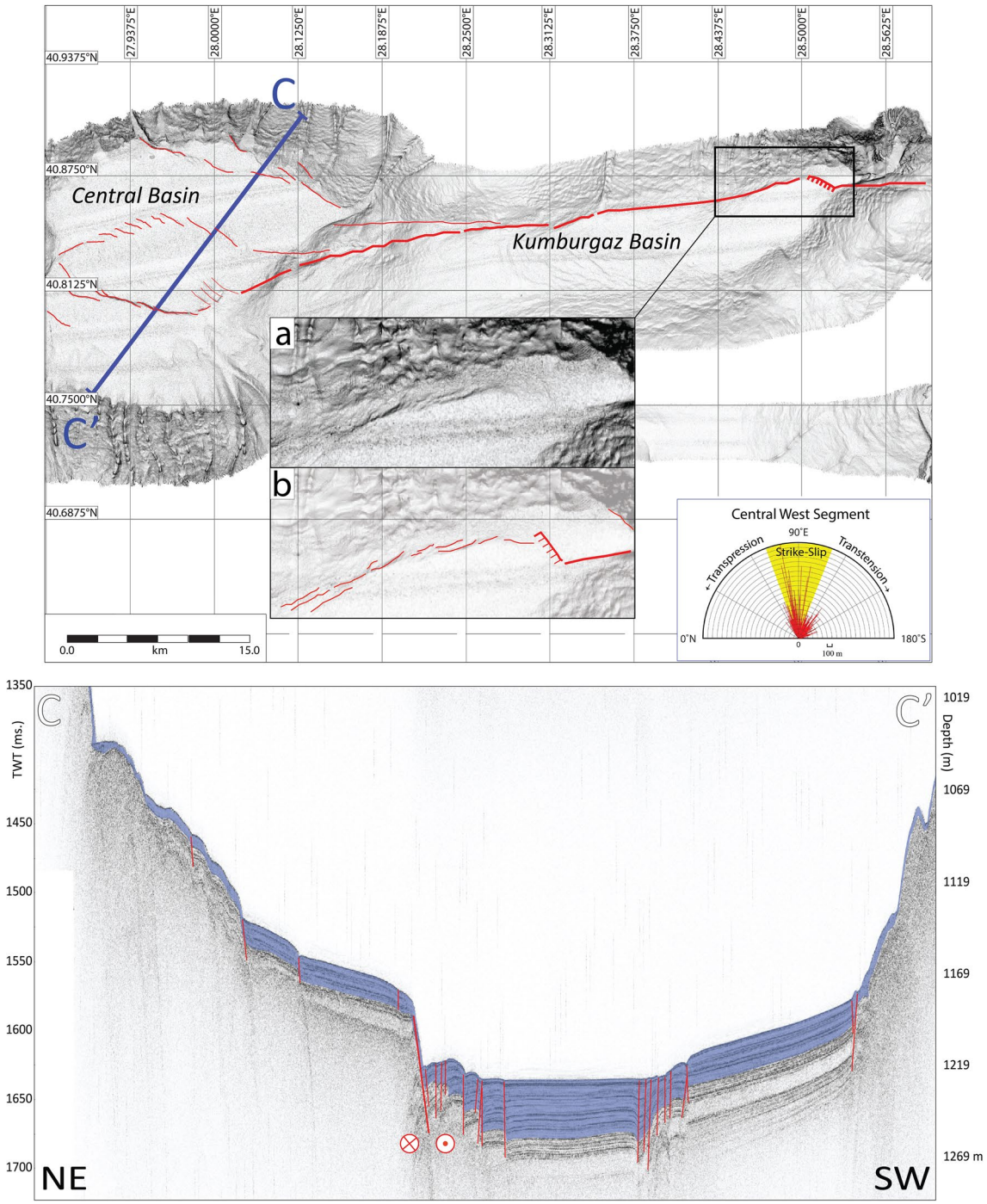

Fig. 7 Morphostructures along the Central West Segment. Top: slope-map of the seafloor obtained using high-resolution bathymetric data, with main active faults indicated (red coded lines); inset includes a rose-diagram representing active fault segments orientations. Bottom: high-resolution seismic reflection profile (section A-A' in map) with Holocene sediments (pale-blue pattern) and active fault segments indicated. Insets include a close-up view of the seafloor morphology **a** with main fault tracks **b**

Our analysis was carried out considering fault activity during the Holocene (10 ka) because its base is identified in the Sea of Marmara by a characteristic unconformity (Çağatay et al. 2001; Polonia et al. 2004). Moreover, given that the average recurrence time of large magnitude earthquakes (Mw > 7) over a single segment of the NAF is around 250–300 years (Ambraseys and Finkel 1990; Ambraseys 2002; Rockwell et al. 2009; Meghraoui et al. 2012), a time span of 10 ka should include several

earthquake cycles and is thus representative of the long-term behavior of the fault.

The first-order segmentation of the NAF in the Sea of Marmara shown by our analysis has important implications for seismic hazard assessments in the densely populated region of the Istanbul metropolitan area. Using the newly compiled neotectonic map of Fig. 4 and the Wells and Coppersmith (1994) relationships we estimated the seismogenic potential of each individual fault segment (Table 2; Fig. 9). It ranges from 6.8 to 7.1, in the Central East and the Central West segments, respectively, while considering these two segments as a single element, we obtain an Mw = 7.4. Concerning the other two segments, we obtain Mw = 6.9 and 7.1 for Mw = 7.1 for the Cinarcik and Tekirdag segments, respectively.

These estimates have to be considered "worst case scenarios", since they imply that the entire segments would rupture during a single event.

5 Discussion

Our geophysical data provide high-resolution images of the shallow structural development along the NAF system in the Sea of Marmara, considering shallow deformations as an evidence of fault behavior in the seismogenic zone. Combining high-resolution morpho-bathymetric and seismic reflection data allowed to recognize the active fault segments, often associated with deformation patterns at the seafloor (scarps, reflector offsets, basin depocenters, structural highs, etc.). We were able to verify that, given the high rates of active deformation relative to sediment supply, most tectonic structures have a morphological expression at the seafloor, enabling correlations between adjacent segments, not always trivial in wrench tectonic domains.

According to geodetic estimate (Flerit et al. 2003), the present-day slip rate along main strike-slip segments, which includes coseismic and postseismic displacement during major and minor earthquakes, as well as inter-seismic creeping (Yamamoto et al. 2019) along the northern NAF strand below the Sea of Marmara, should be around 20 mm/year. This is not in agreement with paleoseismological observations that provide estimates of 10 mm/year, on both sides of the Marmara fault system (Gasperini et al. 2011b). Such discrepancies (or at least part of them) could be reconciled by mechanical models such as that proposed by Hegert and Heidbach (2010), which obtained slip rates between 12.8 and 17 mm/year along the active segments in the Sea of Marmara.

In the 10 ka time scale, a rough estimate that would consider the coseismic component alone, and a maximum 4–5 m of lateral displacement for each Mw > 7 events, as observed during the 1999 Izmit earthquake (Çakir et al. 2003), we obtain an average recurrence period of about 250 years assuming an average slip rate of 20 mm/year that becomes 500 years assuming a rate of 10 mm/year. How does such recurrence intervals fit with historical catalogues and paleoseismic records deduced from the study of sediment cores?

Regarding historical catalogues, suffering high uncertainties in the epicenter locations, we should limit our discussion to the post 1509 C.E. event, which, according to most analyses, should be located along the Cinarcik segment. There is general agreement that the subsequent 1719 event is similar to the 1999 Izmit earthquake and that the 1766 Aug event correlates with the 1912 Ganos-Murefte earthquake, which most probably ruptured at least part of the Tekirdag segment. It remains to locate the 1754 (most probably to the west of Izmit), the 1766 May and the 1894. A key point is where we could locate the 1766 May, or in other words, whether it ruptured the Cinarcik, or one (or both) of the two Central segments. If it was on the Cinarcik segment, is it reasonable to assume that the 1894 event also ruptured that segment 130 years later? Or did the latter rupture the southern NAF branches? Available data do not allow answering these questions unambiguously.

A major point arises from comparative analysis of our new potential magnitudes and historical earthquakes. In fact, the latter appear higher than those predicted by the Wells and Coppersmith (1994) empirical formulas on our segments. However, uncertainties about the historical epicenter determination and magnitudes do not allow for univocal association of major historical earthquakes to any specific fault segment in the Sea of Marmara, with the obvious exclusion of the Izmit 1999 and the Ganos-Murefte 1912 events.

Paleoseismic studies carried out on sediment cores have the potential of longer time records. In particular, the 28 seismoturbidites observed during the past 6.1 kyrs. in the Kumburgaz basin (Yakupoğlu et al. 2019) provide an average recurrence time interval of ~ 220 years., while eight major earthquakes during the past 2400 years. in the Gulf of Izmit provide an average recurrence time of about 300 years. However, the intervals between consecutive events are highly variable, ranging from 90 to 695 yrs. (Çağatay et al. 2012).

For the Cinarcik basin Drab et al. (2015) suggest that the most recent turbidite was triggered by the 1894 C.E. Mw 7.3 earthquake and that the Çınarcık segment ruptured in 1509 C.E., sometime in the fourteenth century, in 989 C.E., and in 740 C.E., with a mean recurrence interval in the range of 256–321 years.

Regarding the Western and Central basins, Drab et al. (2012) recognize eight major turbiditic events in the Tekirdag Basin and seven in the Central Basin during the past 2500 years, which gives a recurrence interval of about 300–350 years. It is worth noting, however, that large-magnitude events could produce effects in different basins.

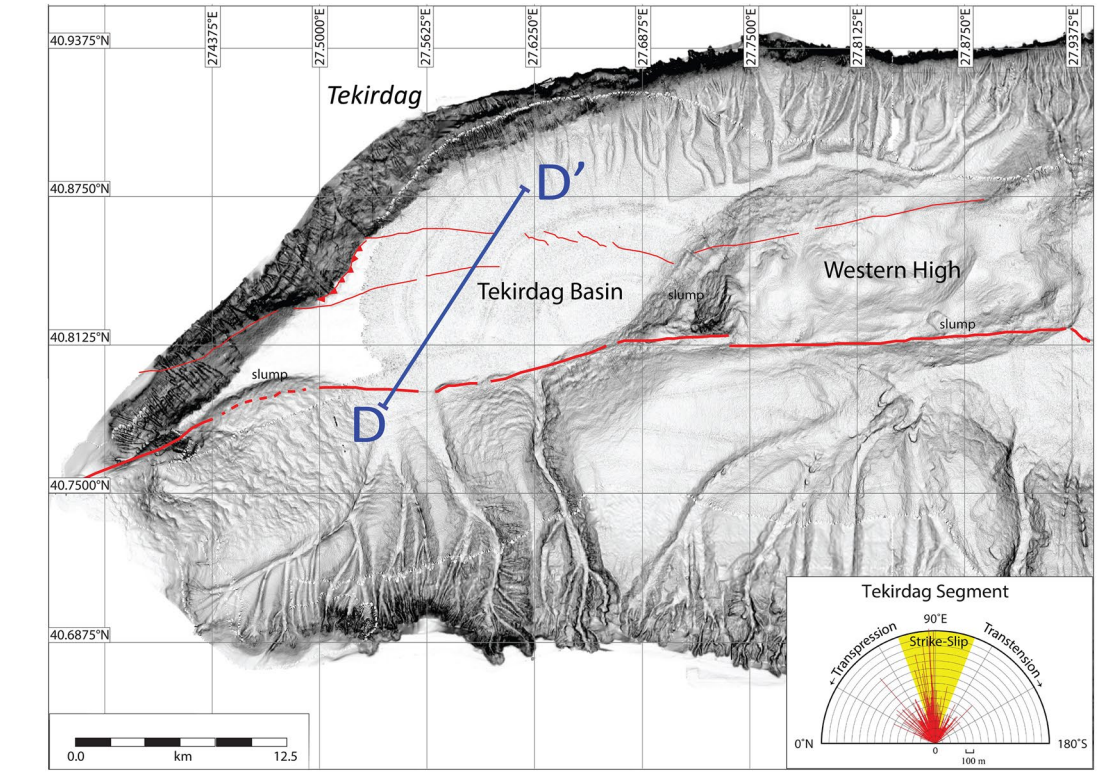
40.9375°N
40.8750°N
40.8125°N
40.7500°N
40.6875°N
27.4375°E
27.5000°E
27.5625°E
27.6250°E
27.6875°E
27.7500°E
27.8125°E
27.8750°E
27.9375°E
Tekirdag
D'
D
Tekirdag Basin
Western High
slump
slump
slump
0.0
km
12.5
Tekirdag Segment
90°E
Transpression
Strike-Slip
Transtension
0°N
180°S
0
100 m

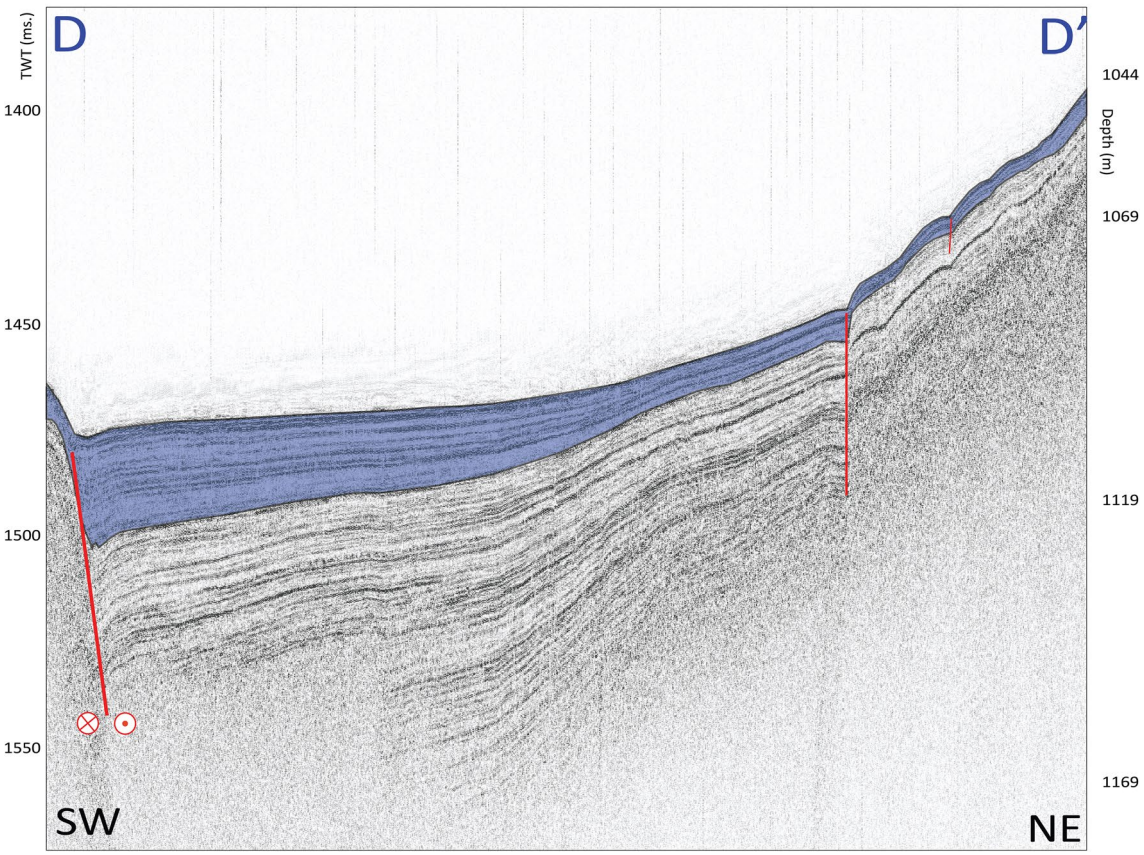
D
D'
TWT (ms.)
1400
1450
1500
1550
Depth (m)
1044
1069
1119
1169
SW
NE

◂**Fig. 8** Morphostructures along the Tekirdag Segment. Top: slope-map of the seafloor obtained using high-resolution bathymetric data, with main active faults indicated (red coded lines); inset includes a rose-diagram representing active fault segments orientations. Bottom: high-resolution seismic reflection profile (section A-A' in map) with Holocene sediments (pale-blue pattern) and active fault segments indicated

We conclude that, although an average recurrence time of 250–350 years for each segment is compatible with most observations, no clear reconstructions of the Holocene earthquake record are available to date for the Sea of Marmara, particularly concerning attribution of a specific earthquake to a given segment. The newly compiled morphotectonic map could represent a starting point for further paleoseismic studies in the region.

6 Conclusions

A newly compiled morphobathymetric map of the North-Anatolian Fault below the Sea of Marmara was presented in this work. Our reconstruction is based on an unpublished morpho-bathymetric and seismic reflection dataset in conjunction with all available data collected starting from 1999. Analysis of this map, discussed considering information deduced from historical and paleoseismic data, led us to the following conclusions:

(1) The right-lateral strike-slip domain characterizing the North-Anatolian fault system shows in the Sea of Marmara three types of deformation, which include almost purely strike-slip faults, mainly oriented E–W; NE/SW-aligned axes of transpressive structures; NW/SE-oriented trans-tensional depressions. This general rule has an exception, i.e., the extensional part of the Tekirdag segment in the westernmost basin edge. This is possibly due to inherited structures and to the progressive counterclockwise rotations of the Anatolia-Eurasia relative motion vectors towards the west.
(2) Segmentation occurs at different scales, but main segments develop along three major right-lateral oversteps, which delimit main fault branches; from east to west: the transtensive Cinarcik segment; the Central (East and West) segments; and the westernmost Tekirdag segment.
(3) If we consider the Central E and W a single rupturing fault, the minimum potential for generating strong earthquakes is along the Cinarcik segment, which is mostly extensional and located between the Central Marmara region and the Izmit segment to the west that has ruptured entirely in 1999, with an estimated magnitude as high as 7.6.
(4) Magnitudes larger than Mw = 7 are possible in the Central segment (E + W);
(5) In light of observation of recentmost events, the Tekirdag segment, with lower estimated magnitudes, should have ruptured in the past (and could rupture in the future) together with the Ganos segment onshore.

We stress the many uncertainties still present in historical and paleoseismic reconstructions for the Marmara Region, particularly evident thanks to this improved knowledge of position and kinematics of active tectonic structures. This gap could be filled by further studies, which should mostly deal with that valuable piece information stored in the sedimentary sequence of the Sea of Marmara. Combining such studies with an improved analysis of historical information would allow calibration of paleoseismic records and refine the 10 ka time-scale record, providing a robust framework to formulate a reliable seismic risk assessment.

Table 2 Maximum expected magnitudes along the fault segments of the NAF below the Sea of Marmara according to this analysis and to Wells and Coppersmith (1994) empirical relationships

	Cinarcik segment				
Length (Km)	Kinematics	Log (L)	*a*	*B*	*M*
32.19	N	1.507721	4.86	1.32	6.9
	Central east segment				
Length (Km)	Kinematics	Log (L)	*a*	*B*	Mw
30.75	SS	1.4878451	5.16	1.12	6.8
	Central west segment				
Length (Km)	Kinematics	Log (L)	*a*	*B*	Mw
36.344	SS	1.5604327	5.16	1.12	6.9
10.42	SS	1.0178677	5.16	1.12	6.3
12.685	SS	1.1032905	5.16	1.12	6.4
59.449	SS (total)	1.7741446	5.16	1.12	7.1
	Central (E + W)				
Length (Km)	Kinematics	Log (L)	*a*	*B*	Mw
90.199	SS (total)	1.9552017	5.16	1.12	7.4
	Tekirdag segment				
Length (Km)	Kinematics	Log (L)	*a*	*B*	Mw
51.91	SS (total)	1.715251	5.16	1.12	7.1
Wells and Coppersmith (1994)				*N* = Normal	
	$M = a + b$*Log(L)			*SS* = Strike-slip	

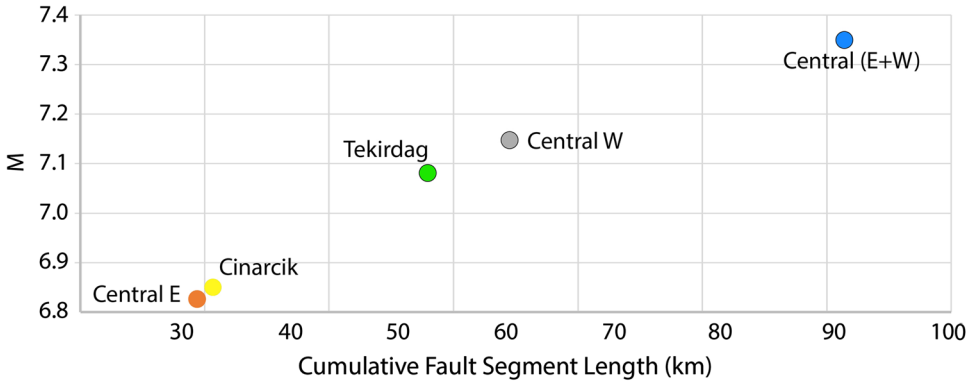

Fig. 9 Cumulative lengths vs Maximum expected magnitudes of fault segments along the NAF below the Sea of Marmara, according to this analysis and Wells and Coppersmith (1994) empirical relationships

Acknowledgements We thank officers and crew of R/V Urania and scientific MARMARA2013 cruise for their cooperation during fieldwork. Comments and suggestions of the Editor and two anonymous referees greatly improved the quality of the manuscript.

Compliance with ethical standards

Conflict of interest On behalf of all authors, the corresponding author states that there is no conflict of interest.

References

Aksoy ME, Meghraoui M, Vallée M, Çakır Z (2010) Rupture characteristics of the A.D. 1912 Mürefte (Ganos) earthquake segment of the North Anatolian fault (western Turkey). Geology 11:991–994. https://doi.org/10.1130/G31447.1

Aksu AE, Calon TJ, Hiscott RN, Yasar D (2000) Anatomy of the North Anatolian Fault Zone in the Marmara Sea, Western Turkey: extensional basins above a continental transform. Gsa Today 10(6):3–7

Ambraseys NN (2002) The seismic activity of the Marmara Sea region over the last 2000 years. Bull Seismol Soc Am 92:1–18. https://doi.org/10.1785/0120000843

Ambraseys N, Finkel C (1990) The Marmara Sea earthquake of 1509. Terra Nova 2:167–174

Ambraseys NN, Finkel C (1991) Long-term seismicity of Istanbul and of the Marmara Sea region. Terra Nova 3:527–539

Ambraseys N, Finkel C (1995) The seismicity of Turkey and adjacent areas 1500–1800. Eren Yayıncılık ve Kitapcılık, Turkey, p 240

Ambraseys NN, Jackson JA (2000) Seismicity of the Sea of Marmara (Turkey) since 1500. Geophys J Int 141:F1–F6

Armijo R, Meyer B, Navarro S, King G, Barka A (2002) Asymmetric slip partitioning in the Sea of Marmara pull-apart: a clue to propagation processes of the North Anatolian Fault. Terra Nova 14(2):80–86

Armijo R, Pondard N, Meyer B, Ucarkus G, De LBM, Malavieille J, Dominguez S, Gustcher M-A, Schmidt S, Beck C, Çağatay N, Cakir Z, Imren C, Eris K, Natalin B, Ozalaybey S, Tolun L, Lefevre I, Seeber L, Gasperini L, Rangin C, Emre O, Sarikavak K (2005) Submarine fault scarps in the Sea of Marmara pull-apart (North Anatolian Fault): implications for seismic hazard in Istanbul. Geochem Geophys Geosyst 6:Q06009. https://doi.org/10.1029/2004GC000896

Atakan K, Ojeda A, Meghraoui M, Barka AA, Erdik M, Bodare A (2002) Seismic hazard in Istanbul following the 17 August 1999 Izmit and 12 November 1999 Duzce earthquakes. Bull Seismol Soc Am 92(1):466–482

Bakun WH, Wentworth CM (1997) Estimating earthquake location and magnitude from seismic intensity data. Bull Seismol Soc Am 87:1502–1521

Barka AA (1992) The North Anatolian fault zone. Ann Tecton 6:164–195

Barka AA, Kadinsky-Cade K (1988) Strike-slip fault geometry in Turkey and its influence on earthquake activity. Tectonophysics 7:663–684

Beck et al (2007) Late Quaternary co-seismic sedimentation in the Sea of Marmara's deep basins. Sed Geol 199:65–89

Bohnhoff M, Bulut F, Gresen G, Malin P, Eken T, Aktar M (2013) An earthquake gap south of Istanbul. Nat Commun 4:1999. https://doi.org/10.1038/ncomms2999

Bulkan S, Vannucchi P, Gasperini L, Polonia A, Cavozzi C (2020) Modelling tectonic deformation along the North-Anatolian Fault in the Sea of Marmara. Tectonophysics 794:228612. https://doi.org/10.1016/j.tecto.2020.228612

Bulut F, Aktuğ B, Yaltırak C, Doğru A, Özener H (2019) Magnitudes of future large earthquakes near Istanbul quantified from 1500 years of historical earthquakes, present-day microseismicity and GPS slip rates. Tectonophysics 764:77–87. https://doi.org/10.1016/j.tecto.2019.05.005

Çağatay MN, Görür N, Algan O, Eastoe C, Tchapalyga A, Ongan D, Kuhn T, Kuşcu I (2000) Late Glacial-Holocene palaeoceanography of the Sea of Marmara: timing of connections with the Mediterranean and the Black Seas. Mar Geol 167(3–4):191–206. https://doi.org/10.1016/S0025-3227(00)00031-1

Çağatay MN, Görür N, Polonia A, Demirbağ E, Sakınç M, Cormier MH, Capotondi L, McHugh C, Emre Ö, Eriş K (2003) Sea level changes and depositional environments in the İzmit Gulf, eastern Marmara Sea, during the late glacial-Holocene period. Mar Geol 202:159–173

Çağatay MN, Eriş K, Ryan WBF, Sancar Ü, Polonia A, Akçer S, Biltekin D, Gasperini L, Görür N, Lericolais G, Bard E (2009) Late Pleistocene-Holocene evolution of the northern shelf of the Sea of Marmara. Mar Geol 265:87–100

Çağatay MN, Erel L, Bellucci LG, Polonia A, Gasperini L, Eris KK, Sancar Ü, Biltekin D, Uçarkus G, Ülgen UB, Damci E (2012) Sedimentary earthquake records in the Izmit Gulf, Sea of Marmara, Turkey. Sed Geol 282:347–359. https://doi.org/10.1016/j.sedgeo.2012.10.001

Çakir Z et al (2003) Coseismic and early post-seismic slip associated with the 1999 Izmit earthquake (Turkey), from SAR interferometry and tectonic field observations. Geophys J Int 155(1):93–110. https://doi.org/10.1046/j.1365-246X.2003.02001.x

Dal Forno G, Gasperini L (2008) ChirCor: a new tool for generating synthetic chirp-sonar seismograms. Comput Geosci 34(2):103–114

Drab L, Hubert-Ferrari A, Schmidt S, Martines P (2012) The earthquake sedimentary record in the western part of the Sea of Marmara Turkey. Nat Hazards Earth Syst Sci 12:1235–1254. https://doi.org/10.5194/nhess-12-1235-2012

Drab L, Hubert-Ferrari A, Schmidt S, MartinesCarlut PJ, El Ouahabi M (2015) Submarine Earthquake History of the C narc k Segment of the North Anatolian Fault in the Marmara Sea, Turkey. Bull Seismol Soc Am 105(2A):622–645

Ergintav S et al (2014) Istanbul's earthquake hot spots: geodetic constraints on strain accumulation along faults in the Marmara seismic gap. Geophys Res Lett 41:5783–5788

Eris KK, Ryan WBF, Çağatay MN, Sancar U, Lericolais G, Ménot G, Bard E (2007) The timing and evolution of the post-glacial transgression across the Sea of Marmara shelf south of İstanbul. Mar Geol 243(1–4):57–76. https://doi.org/10.1016/j.margeo.2007.04.010

Flerit F, Armijo R, King GCP, Meyer B, Barka A (2003) Slip partitioning in the Sea of Marmara pull-apart determined from GPS velocity vectors. Geophys J Int 154(1):1–7

Gasperini L, Stanghellini G (2009) SeisPrho: an interactive computer program for processing and interpretation of high-resolution seismic reflection profiles. Comput Geosci 35:1497–1507. https://doi.org/10.1016/j.cageo.2008.04.014

Gasperini P, Bernardini F, Valensise G, Boschi E (1999) Defining seismogenic sources from historical felt reports. Bull Seismol Soc Am 89:94–110

Gasperini P, Vannucci G, Tripone D, Boschi E (2010) The location and sizing of historical earthquakes using attenuation of macroseismic intensity with distance. Bull Seismol Soc Am 100:2035–2066. https://doi.org/10.1785/0120090330

Gasperini L, Polonia A, Bortoluzzi G, Henry P, Le Pichon X, Tryon M, Çağatay MN, Geli L (2011a) How far did the surface rupture of the 1999 Izmit earthquake reach in Sea of Marmara? Tectonics 30:TC1010. https://doi.org/10.1029/2010TC002726

Gasperini L, Polonia A, Çağatay MN, Bortoluzzi G, Ferrante V (2011b) Geological slip rates along the North Anatolian fault in the Marmara region. Tectonics 30:TC6001. https://doi.org/10.1029/2011TC002906

Gasperini L et al (2013) (2013) Marmara 2013 cruise report. Novembre, ISMAR-BO Cruise Reports, p 51

Gasperini L, Polonia A, Çağatay MN (2018) Fluid flow, deformation rates and the submarine record of major earthquakes in the Sea of Marmara, along the North-Anatolian Fault system. Deep Sea Res Part II. Top Stud Oceanogr 153:4–16

Gomez Capera AA, Meletti C, Musson R, Stucchi M (2009) The European Earthquake Catalogue (1000–1600), demo version. Part 1—The NA4 Calibration Initiative. NA4 deliverable D5,

NERIES Project. http://emidius.mi.ingv.it/neries_NA4/docs/NA4_D5.pdf
Hergert T (2010) Heidbach O (2010) Slip-rate variability and distributed deformation in the Marmara Sea fault system. Nature Geosciences 3:132–135
Hubert-Ferrari A, Barka A, Jacques E, Nalbant S, Meyer B, Armijo R, Tapponier P, King GCP (2000) Seismic hazard in the Marmara Sea following the 17 August 1999 Izmit earthquake. Nature 404:269–272
Lange D, Kopp H, Royer JY, Henry P, Cakir Z, Petersen F, Geli L (2019) Interseismic strain build-up on the submarine North Anatolian fault offshore Istanbul. Nat Commun 10(1):9. https://doi.org/10.1038/s41467-019-11016-z
Geli et al (2009) Marmesonet Leg I. Cruise report. Nov 4th–Nov 25th, 2009.
Le Pichon X, De LBM, Meyer B, Armijo R, Go N, Saatc R, Tok B (2001) The active Main Marmara fault. Earth Planet Sci Lett 192(4):595–616. https://doi.org/10.1016/S0012-821X(01)00449-6
McClusky S, Balassanian S, Barka A, Demir C, Ergintav S, Georgiev I, Gürkan O, Hamburger M, Hurst K, Kahle H, Kastens K, Kekelidze K, King R, Kotzev V, Lenk O, Mahmoud S, Mishin A, Nadariya M, Ouzounis A, Paradissis D, Peter Y, Prilepin M, Reilinger R, Sanlı I, Seeger H, Tealeb A, Toksöz MN, Veis G (2001) Global positioning system constraints on plate kinematics and dynamics in the eastern Mediterranean and Caucasus. J Geophys Res 105:5695–5719
McHugh CMG, Seeber L, Cormier M-H, Dutton J, Çağatay MN, Polonia A, Ryan WBF, Gorur N (2006) Submarine earthquake geology along the North Anatolia Fault in the Marmara Sea, Turkey: a model for transform basin sedimentation. Earth Planet Sci Lett 248:661–684
McHugh CMG, Gurung D, Giosan L, Ryan WBF, Mart Y, Sancar U, Burckle L, Çağatay MN (2008) The last reconnectionof the Marmara Sea (Turkey) to the World Ocean: a paleoceanographic and paleoclimatic perspective. Mar Geol 255:64–82
Meghraoui M, Aksoy ME, Akyüz HS, Ferry M, Dikbaş A, Altunel E (2012) Paleoseismology of the North Anatolian Fault at Güzelköy (Ganos segment, Turkey): size and recurrence time of earthquake ruptures west of the Sea of Marmara. Geochem Geophys Geosyst 13:Q04005. https://doi.org/10.1029/2011GC003960
Meral Ozel N, Necmioglu O, Ergintav S, Ozel A, Erdik MO (2013) MARSite: Marmara as a Supersite. American Geophysical Union, Fall Meeting 2013, abstract id. NH13B-1619
Okay AI, Kaslilar-Ozcan A, Imren C, Boztepe-Guney A, Demirbag E, Kuscu I (2000) Active faults and evolving strike-slip fault basins in the Marmara Sea, northwest Turkey: a multichannel reflection study. Tectonophysics 312:189–218
Parke JR, White RS, McKenzie D, TA, Minshull, JM, Bull, I, Kuscu, N, Gorur, C, Sengor (2002) Interaction between faulting and sedimentation in the Sea of Marmara, western Turkey. J Geophys Res 107(B11):2286. https://doi.org/10.1029/2001JB000450
Parsons TS (2004) Recalculated probability of M>7 earthquakes beneath the Sea of Marmara. J Geophys Res 109:B05304. https://doi.org/10.1029/2003JB002667
Parsons TS, Toda TS, Stein RS, Barka AA, Dietrich JH (2000) Heightened odds of large earthquakes near Istanbul: An interaction-based probability calculation. Science 288:661–665. https://doi.org/10.1126/science.288.5466.661
Polonia A et al (2002) Exploring submarine earthquake geology in the Marmara Sea. Eos, Trans Am Geophysic Union 83:229–236
Polonia A, Gasperini L, Amorosi A, Bonatti E, Çağatay N, Capotondi L, Cormier M-H, Gorur N, McHugh C, Seeber L (2004) Holocene slip rate of the North Anatolian Fault beneath the Sea of Marmara. Earth Planet Sci Lett 227:411–426. https://doi.org/10.1016/j.epsl.2004.07.042
Reilinger R, McClusky S, Vernant P, Lawrence S, Ergintav S, Cakmak R, Ozener H, Kadirov F, Guliev I, Stepanyan R et al (2006) GPS constraints on continental deformation in the Africa–Arabia–Eurasia continental collision zone and implications for the dynamics of plate interactions. J Geophys Res 111:B05411
Rockwell TK et al (2009) Palaeoseismology of the North Anatolian Fault near the Marmara Sea: Implications for fault segmentation and seismic hazard. In: Reicherter K, Michetti AM, Silva PG (eds) Palaeoseismology: historical and prehistorical records of earthquake ground effects for Seismic Hazard Assessment. Geol Soc Spec Publ. 316:31–54. https://doi.org/10.1144/SP316.3
Şengör (2003) The North Anatolian fault in the Sea of Marmara. J Geophys Res 108(B4):2179. https://doi.org/10.1029/2002JB001862
Şengör AMC, Grall C, İmren C, Le Pichon X, Görür N, Henry P, Karabulut H, Siyako M (2014) The geometry of the North Anatolian transform fault in the Sea of Marmara and its temporal evolution: Implications for the development of intracontinental transform faults. Can J Earth Sci 51(3):222–242
Sperling M, Schmiedl G, Hemleben Ch, Emeis KC, Erlenkeuser H, Grootes PM (2003) Black Sea impact on the formation of eastern Mediterranean sapropel S1? Evidence from the Marmara Sea. Palaeogeogr Palaeoclimatol Palaeoecol 190:9–21
Stucchi M, Rovida A, Gomez Capera AA, Alexandre P, Camelbeeck T, Demircioglu MB, Gasperini P, Kouskouna V, Musson RMW, Radulian M, Sesetyan K, Vilanova S, Baumont D, Faeh D, Lenhardt W, Makropoulos K, Martinez Solares JM, Scotti O, Zivcic M, Albini P, Batllo J, Papaioannou Ch, Tatevossian R, Locati M, Meletti C, Viganò D, Giardini D (2013) The SHARE European Earthquake Catalogue (SHEEC) 1000–1899. J Seismol 17:523–524. https://doi.org/10.1007/s10950-012-9335-2
Ucarkus G, Cakir Z, Armijo R (2011) Western termination of the Mw 7.4, 1999 Izmit earthquake rupture: implications for the expected large earthquake in the Sea of Marmara. Turkish J Earth Sci 20:383–398
Vidal L, Menot G, Joly C, Bruneton H, Rostek F, Çağatay MN, Major C (2010) Hydrology in the Sea of Marmara during the last 23 ka: implications for timing of Black Sea connections and sapropel deposition. Paleoceanography (in press). https://doi.org/10.1029/2009PA001735
Wells D, Coppersmith K (1994) New empirical relationships among magnitude, rupture length, rupture width, rupture area, and surface displacement. Bull Seismol Soc Am 84:974–1002
Wesnousky SG (2006) Predicting the endpoints of earthquake ruptures. Nature 444(7117):358–360
Wessel P, Smith WHF (1991) Free software helps map and display data. Eos Trans Am Geophys Union 72(41):441–446. https://doi.org/10.1029/90EO00319
Wong HK, Luedmann T, Ulug A, Gorur N (1995) The Sea of Marmara: a plate boundary sea in an escape tectonic regime. Tectonophysics 244:231–250
Yakupoğlu N, Uçarkuş G, Eriş KK, Henry P, Çağatay MN (2019) Sedimentological and geochemical evidence for seismoturbidite generation in the Kumburgaz Basin, Sea of Marmara: Implications for earthquake recurrence along the Central High Segment of the North Anatolian Fault. Sed Geol 380:31–44. https://doi.org/10.1016/j.sedgeo.2018.11.002
Yamamoto R, Kido M, Ohta Y, Takahashi N, Yamamoto Y, Pinar A, Kalafat D, Özener H, Kaneda Y (2019) Seafloor Geodesy revealed partial creep of the North Anatolian Fault Submerged in the Sea of Marmara. Geophys Res Lett 46(3):1268–1275